Polarization switching and patterning in self-assembled peptide tubular structures

Igor Bdikin, Vladimir Bystrov, Ivonne Delgadillo, José Gracio, Svitlana Kopyl et al.

Related Articles

A variational formulation of electrostatics in a medium with spatially varying dielectric permittivity
J. Chem. Phys. 138, 054119 (2013)

The x-ray absorption spectroscopy model of solvation about sulfur in aqueous L-cysteine
JCP: BioChem. Phys. 6, 11B620 (2012)

The x-ray absorption spectroscopy model of solvation about sulfur in aqueous L-cysteine
J. Chem. Phys. 137, 205103 (2012)

Extremely slow photocurrent response from hemoprotein films in planar diode geometry
Appl. Phys. Lett. 101, 223701 (2012)

Dielectric spectra broadening as a signature for dipole-matrix interaction. III. Water in adenosine monophosphate∕adenosine-5′-triphosphate solutions
JCP: BioChem. Phys. 6, 11B613 (2012)

Additional information on J. Appl. Phys.

Journal Homepage: http://jap.aip.org/
Journal Information: http://jap.aip.org/about/about_the_journal
Top downloads: http://jap.aip.org/features/most_downloaded
Information for Authors: http://jap.aip.org/authors

Polarization switching and patterning in self-assembled peptide tubular structures

Igor Bdikin,[1] Vladimir Bystrov,[2,3,a)] Ivonne Delgadillo,[4] José Gracio,[1] Svitlana Kopyl,[1] Maciej Wojtas,[2] Elena Mishina,[5] Alexander Sigov,[5] and Andrei L. Kholkin[2,b)]

[1]*Department of Mechanical Engineering & TEMA, University of Aveiro, 3810-193 Aveiro, Portugal*
[2]*Department of Ceramics and Glass Engineering & CICECO, University of Aveiro, 3810-193 Aveiro, Portugal*
[3]*Institute of Mathematical Problems of Biology RAS, Puschino, 142290 Moscow District, Russia*
[4]*Department of Chemistry & QOPNA, University of Aveiro, 3810-193, Aveiro, Portugal*
[5]*Moscow State Institute of Radioengineering, Electronics and Automation, 119454 Moscow, Russia*

Self-assembled peptide nanotubes are unique nanoscale objects that have great potential for a multitude of applications, including biosensors, nanotemplates, tissue engineering, biosurfactants, etc. The discovery of strong piezoactivity and polar properties in aromatic dipeptides [A. Kholkin, N. Amdursky, I. Bdikin, E. Gazit, and G. Rosenman, ACS Nano **4**, 610 (2010)] opened up a new perspective for their use as biocompatible nanoactuators, nanomotors, and molecular machines. Another, as yet unexplored functional property is the ability to switch polarization and create artificial polarization patterns useful in various electronic and optical applications. In this work, we demonstrate that diphenylalanine peptide nanotubes are indeed electrically switchable if annealed at a temperature of about 150 °C. The new orthorhombic antipolar structure that appears after annealing allows for the existence of a radial polarization component, which is directly probed by piezoresponse force microscopy (PFM) measurements. Observation of the relatively stable polarization patterns and hysteresis loops via PFM testifies to the local reorientation of molecular dipoles in the radial direction. The experimental results are complemented with rigorous molecular calculations and create a solid background of electric-field induced deformation of aromatic rings and corresponding polarization switching in this emergent material. © *2012 American Institute of Physics*. [http://dx.doi.org/10.1063/1.3699202]

I. INTRODUCTION

The ordering of molecular dipoles and ferroelectricity in organic materials are becoming increasingly important in view of novel opportunities offered in the areas of microelectronics and microelectromechanical systems, especially for ferroelectric field effect transistors and non-volatile memories.[1,2] Many organic biomaterials, including proteins, peptides, amino acids, and polysaccharides, have highly organized molecular dipole assemblies and are frequently piezoelectric due to the presence of polar bonds and natural asymmetry. Some biomolecules with bias-induced conformational states also possess true ferroelectric properties.[3] These organic materials having spontaneous polarization created by complex supramolecular assemblies are also important building blocks in modern nanotechnology.[4–6] Compared to inorganic ferroelectrics/piezoelectrics, they are far cheaper, and their structure can be easily controlled through chemistry, which makes them highly versatile and flexible. Although not many organic ferroelectric materials have been identified so far, the past decade has seen significant progress in the discovery of new organic ferroelectrics useful for microelectronics.[1,3,7] One of the most interesting materials for nanoelectronic applications belongs to the class of self-assembled peptide nanostructures.[8] Peptide-based systems are of particular importance from a biological point of view as models for ion channels, membranes, amyloid fibrils,

etc.[9–11] In this group of materials, tube-like structures are easily formed by the stacking of aromatic rings through the formation of hydrogen bonds between functional groups in the backbone structure, related to aromatic π-π interactions.[12] A robust self-assembly process in the short aromatic dipeptide NH2-Phe-Phe-COOH was studied in detail by Gorbitz[13–15] and by Gazit's group.[8,11,12,16,17] Recently, it was demonstrated that peptide nanotubes (PNTs) are also strongly piezoelectric with the orientation of polarization along the tube axis.[18] However, previous attempts to switch the polarization in this material were unsuccessful due to the geometry of vertical nanotubes and the extremely high coercive field, which did not allow full polarization switching.[19]

In this paper, we report for the first time persistent polarization switching and bias-induced polarization patterning in diphenylalanine (FF) peptide nanotubes annealed at 150 °C via piezoresponse force microscopy (PFM). We believe that this observation adds a new functionality to this emergent material, with potential applications in solid-state memories, nanoactuators, and nanophotonic devices. The importance of the demonstrated polarization switching in FF PNTs stems also from their connection to β amyloid proteins, the crystallized structures formed with Alzheimer disease.[12]

II. METHODS OF SAMPLE PREPARATION AND MEASUREMENTS

PNTs were prepared by dissolving the FF building blocks in lyophilized form in 1,1,1,3,3,3-hexafluoro-2-propanol at a

a)Address correspondence to bystrov@ua.pt.
b)Address correspondence to kholkin@ua.pt.

concentration of 100 mg/ml. The stock solution was diluted to a final concentration of 2 mg/ml in ddH$_2$O in order for the nanotube self-assembly process to occur. The diluted solution was dried onto a gold coated silicon surface (150 nm Au, 15 nm Cr). The measurements were done with a commercial AFM (Ntegra Prima, NT-MDT) equipped with an external function generator and a lock-in amplifier (see Refs. 18 and 19 for more details). We used doped Si cantilevers with spring constants in the range of 0.02–1 N/m driven at a frequency of 5 kHz.

III. EXPERIMENTAL RESULTS AND DISCUSSION

Fig. 1(a) represents a typical scanning electron microscopy (SEM) image of the horizontal PNTs self-assembled at room temperature on a planar Si substrate coated with gold. As has been shown in the past,[18,19] they demonstrate apparent tubular morphologies and spontaneously self-assemble in a large variety of dimensions and aspect ratios during solution drying. Piezoresponse force microscopy was then applied in order to study the local piezoelectric properties and polarization, as discussed in detail elsewhere.[20] In these measurements, the conducting PFM tip is scanned in a contact mode while an ac voltage is applied between the tip and a counter electrode. The piezoresponse contrast is acquired in the form of the mixed signal $A \cos \varphi$, with A being the amplitude of the piezoelectric vibration and φ being the phase shift between the driving and detected signals.[21] In this way, polarizations with opposite directions exhibit contrasts of opposite signs. Because the vertical PFM did not reveal any radial polarization component, a lateral PFM was used to detect shear vibrations (due to the shear piezoelectric coefficient d_{15}) in the investigated PNTs.[18] The strong shear piezoactivity of FF PNTs [d_{15} of about 60 pm/V (Ref. 18)] is reflected in the PFM contrast (topography with superimposed PFM image) as shown in Fig. 1(b), in which two intergrown tubes are presented. As the scanning was done in the direction intermediate between the polarization directions of both tubes, different contrast is shown with domain wall-like PFM signal reversal at the tube intersection. Piezocontrast also exhibited electromechanical heterogeneity, revealed as regular stripes at an angle of about 45° to the tube axis. This fine structure of the tubes is similar to the sub-fibrillar heterogeneity observed recently in collagen fibers via PFM.[22] A discussion of the internal fine structure of the contrast is

FIG. 2. X-ray diffraction pattern of the crushed PNT powder after annealing at 150 °C for 1 h.

beyond the scope of this paper and is reserved for future publications.

After the PFM imaging, the as-grown tubes were subjected to heating in a tube furnace to a maximum temperature of 150 °C. The heating and cooling rates were about 1 °C/min, and the holding time was about 10 min. Figure 2 is a representative x-ray diffraction (XRD) pattern of the annealed PNTs (crushed into powder) after this high temperature treatment. For as-grown tubes, the hexagonal structure (a = 24.071 Å, c = 5.456 Å, γ = 120°, and $P6_1$ space group; Cambridge Crystallographic Data Centre (CCDC) file number 163 340) was indexed in agreement with our own data and that from the literature.[13,19] The XRD pattern obtained for annealed PNTs is different (Fig. 2), having XRD peaks of broader width after heating. Based on the crystallographic analysis, a new (orthorhombic) structure with a = 5.210 Å, b = 24.147 Å, and c = 41.072 Å was identified.[19] This structure corresponds to the antiparallel orientation of the dipole moments of individual aromatic rings comprising FF PNTs. In addition, the modified structure (having a zero net polarization in the axial direction) allows for a *radial* polarization component as shown below.

The temperature dependence of the tube morphology and the lateral piezoresponse measured *in situ* on as-grown horizontal tubes are presented in detail in Fig. 3. The topography and PFM signal were followed while the tube sample was slowly heated in the PFM setup. We found that the topography of the tubes does not change until 100 °C, and only at temperatures close to 150 °C do the tubes contract by about 10% to 12% relative to their initial height. This finding confirms the occurrence of some structural changes; however, no collapsing of the tubes or integrity loss were documented in our experimental conditions, in contrast to a recent study by Sedman *et al.*[16] The data are more consistent with the published results of SEM and differential thermal gravimetry (DTG) observations of nanotubes heated in an autoclave.[23] These measurements have shown that FF PNTs exhibit DTG peaks (corresponding to a small weight loss of about 15%) at temperatures of ≈50 °C and 140 °C, with the former being due to the evaporation of crystallization water and the latter to the irreversible degradation resulting from diphenylalanine loss. Our measurements also revealed an
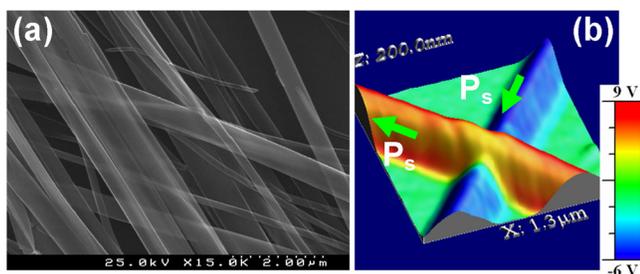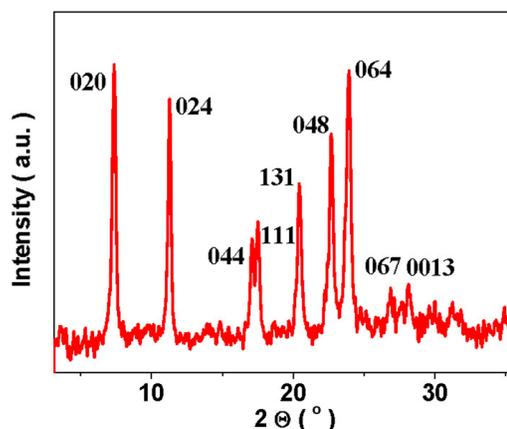

FIG. 1. (a) Representative SEM image of horizontal as-grown peptide nanotubes deposited from the solution. (b) PFM in-plane contrast of intergrown tubes.
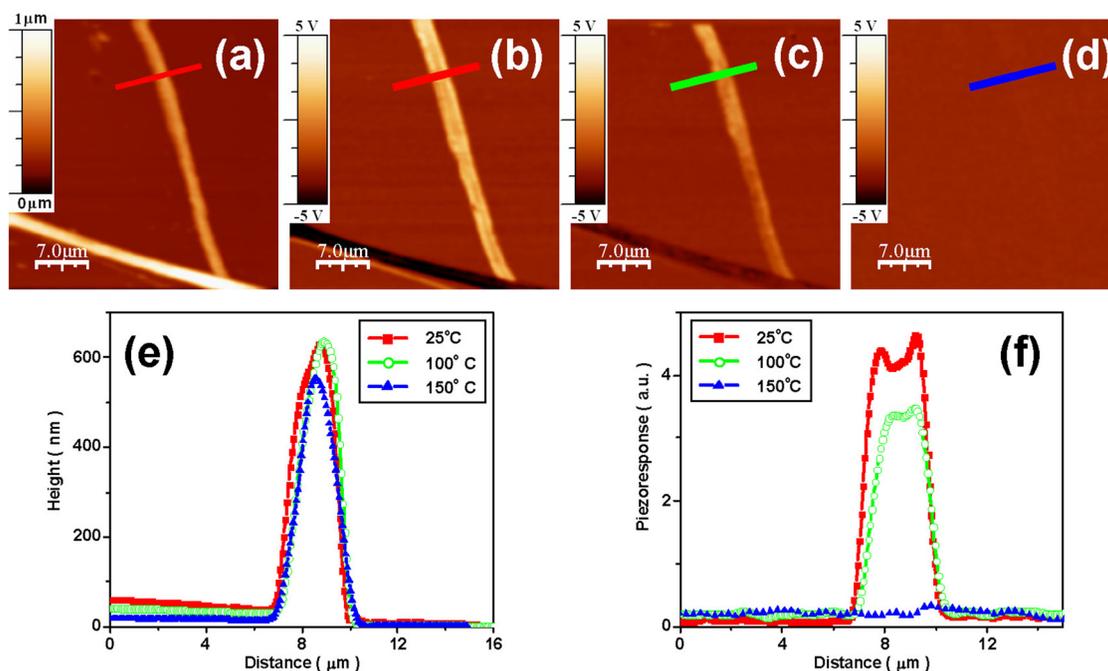
FIG. 3. Temperature dependence of AFM and PFM signals. (a) Topography at 25 °C. (b)–(d) In-plane PFM contrast at 25 °C, 100 °C, and 150 °C, respectively. (e) Comparison of topography cross sections at different temperatures. (f) Comparison of PFM cross sections at different temperatures.

irreversible loss of the piezoresponse contrast that is fully consistent with previous results.[19] The gradual decrease of the piezoresponse signal is attributed to the irreversible structural phase transition from the hexagonal to the ortho-rhombic anti-polar phase allowing a radial component of polarization. It should be mentioned that our data are different from those in the recent report by Ryu and Park,[24] who observed linear-to-cyclic phase transformation with a consequent transition from tube to fiber nanostructure. This happened in an aniline vapor atmosphere via the loss of one molecule of water per one FF.

Following the topography and PFM imaging, the piezoresponse force microscopy was switched from imaging to switching spectroscopy mode so that the PFM signal was acquired at fixed positions under dc bias voltage pulses swept in the range of -100 V $<$ V $<$ $+100$ V. The measurement configuration is schematically shown in Fig. 4(a). No vertical piezoresponse was observed in the as-grown tubes [Fig. 4(b)], even for the high voltage (≈ 90 V) applied in the

radial direction. This is expected in a hexagonal structure, which allows the polarization component to exist only along the axial direction. Surprisingly, annealed tubes demonstrate completely different behavior: clear hysteresis with a threshold-like dependence of the radial piezoresponse at about 30 V. After the first hysteresis, the closed loops were repeatedly acquired, pointing to the robust polarization switching in this material. The loop was quite symmetric, with coercive and nucleation biases of about 60 and 25 to 30 V, respectively. No changes in the PFM signal and topography degradation were observed after the multiple loop acquisition (not shown). The existence of two switchable polarization states is thus confirmed by the PFM measurements in a dynamic regime in which the bias is continuously swept between positive and negative values (i.e., in non-equilibrium conditions[25]). As is well known from the study of ferroelectrics, a high intensity of the inhomogeneous electric field created near the PFM tip strongly reduces the potential barrier and causes domain nucleation and subsequent
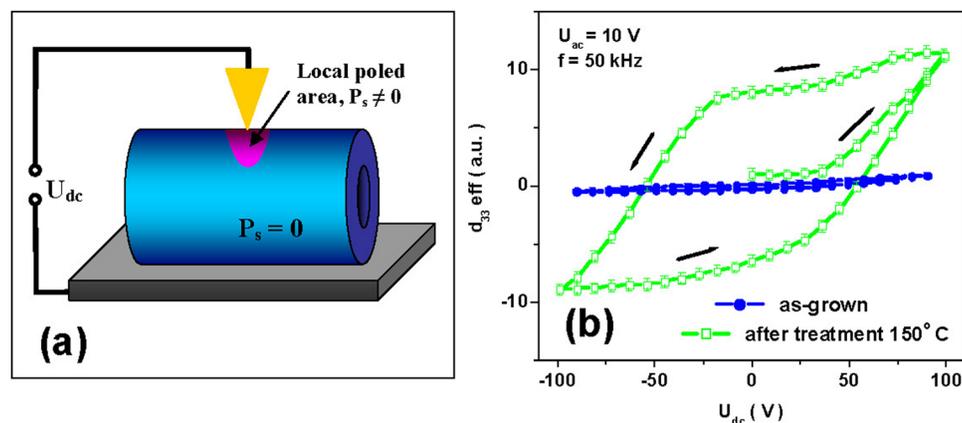

FIG. 4. (a) Schematic of the switching experiment in the radial direction by PFM. (b) Piezoresponse hysteresis of lateral signal in as-grown state and after annealing at 150 °C.
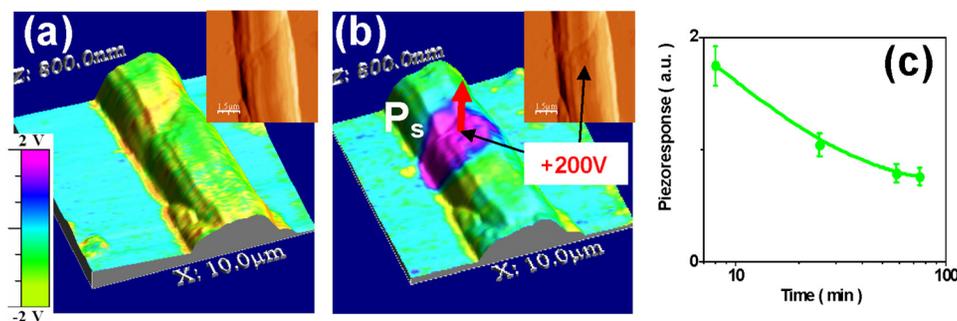
FIG. 5. PFM images of the annealed tubes before (a) and after (b) poling with +200 V over 10 s. (c) Time relaxation of the PFM signal after poling. The insets in (a) and (b) show topography before and after poling.

growth of the ellipsoidal domain into the sample bulk.[26] In equilibrium, the size of the domain depends only on the value of the maximum applied voltage and can be analyzed via phenomenological models.[25] In order to directly visualize the switched polarization and investigate its stability, the positive voltage pulses were applied to fixed locations on the tube surface. Figure 5 shows an example of such a study in which the topography (vertical scale) and piezoresponse (color scale) were obtained before and after the application of a voltage pulse. The topography image demonstrates the full mechanical integrity of the structure (even after poling with high voltage) and the practically vanishing piezoresponse before poling. Local poling resulted in the apparent contrast change of an area about 2 μm in size around the poling point [Fig. 5(b)]. The size of the switched area strongly depended on the poling voltage and poling time, as is typically observed in local switching experiments involving PFM.[27] It should be noted once again that the piezocontrast shown in Fig. 5(b) corresponds to a radial component of the polarization not found in the initial structure arranged as alternating dipoles along the tube axis[19] and was induced by the application of a high bias field, causing apparent rotation of the aromatic rings, as is demonstrated below.

The effect of polarization relaxation after local poling was also studied [Fig. 5(c)]. In this experiment, both negative and positive polarization patterns were written on the same tube for about 10 s. The piezoresponse in the center of the poling area was then measured as a function of time immediately after the poling event. As can be seen from Fig. 5(c), the piezoresponse decays with time by about 50% of its initial value within one time decade. This relaxation is significantly faster than in conventional ferroelectrics[28] and is comparable to that observed in ferroelectric relaxors.[29] Therefore, we used the stretched exponential dependence (Kohlrausch–Williams–Watts-type) frequently applied for systems with dipole–dipole interactions[30] and in ferroelectric relaxors (including local measurements)[29,31]: $(d_{33})_{eff} \sim \exp[-(t/t_0)^b]$, in which t is the time and b and t_0 are the relaxation parameters ($t_0 = 76 \pm 2$ min and $b = 0.50 \pm 0.02$). Thus the measurements demonstrate the sufficiently high stability of the written domains and the apparent slowing down of the polarization decay at long times.

IV. RESULTS OF COMPUTATIONAL MODELING AND DISCUSSION

In order to rationalize the experimental observations and further understand the molecular structure of annealed tubes

enabling a radial component of polarization, we performed molecular simulations of these structures in the virgin state and under radially applied electrical field. Similar to our previous work,[19] we used the commercial package HypeChem 7.52 (Ref. 32) comprising the quantum-chemical semiempirical PM3 technique and molecular mechanical BIO CHARM methods for molecular dynamics runs. It was found that co-operative proton tautomerism[7] and the specific properties of individual FF molecules (e.g., highly mobile torsion angles[13,14] of amino group bonding and easy hydrogen bond N–H…O formation between FF molecules) result in the formation of a dipole moment D (and corresponding polarization P) that lies presumably along the OZ-axis of the hexagonal (i.e., for nonannealed tubes) lattice. The value of the dipole moment D_z is about 40 D, which corresponds to the polarization $P_z = D_z/V \approx 4 \ \mu$C/cm^2, whereas $D_x \approx D_y \approx 0$ [see Fig. S1(a) of the Supplementary Material[40] for more details of the structure]. The peculiarities of the dipole moment formation in the individual FF tube used for modeling are schematically shown in Fig. 6 and Fig. S1(b).[40] In the hexagonal structure, four studied parallel individual FF tubes form a rigid polar structure[19] that is not switchable in either axial or radial directions. In contrast, for the orthorhombic structure (annealed PNTs consisting of the same four aromatic rings), our modeling simulations predict that all P_z's *alternate* in the antipolar fashion and compensate one another, resulting in $P_z \approx 0$ (see details in Fig. 7(a) and the Supplementary Material[40]). At the same time, under radially applied electric field an uncompensated dipole moment appears in the XOY plane, leading to a notable polarization and corresponding radial (vertical) PFM signal. The aromatic rings and corresponding polarizations under electric field are schematically represented in Fig. 7(a) (see also Fig. S2 and Tables S1 and S2 in the Supplementary Material[40]). Figure 7(b) shows the calculated remanent polarization hysteresis loop generated by our molecular model in the presence of an external electric field. The modeling results are in qualitative agreement with the experimental piezoresponse versus voltage dependence [Fig. 4(a)]. The calculation results give only approximate values due to a very complex potential energy surface and odd behavior of the FF torsion angles.[13,14] In this respect, the complex transformation of the studied system in the applied radial electric field is similar to the unwinding of super-helical molecules (see Fig. S2 and Table S1 of the Supplementary Material[40]). But, as evidenced by the loop shape [Fig. 7(b)], the proposed model can still reproduce the salient features of the radial polarization
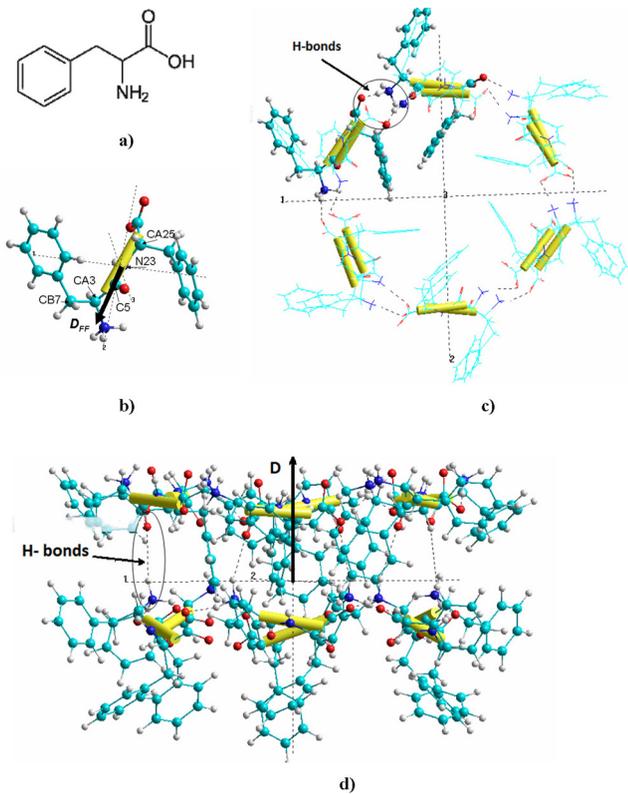
FIG. 6. Formation of total polarization along the OZ axis in FF PNTs for a molecular model with an initial state of 2 FF rings: (a) configuration of a single F molecule containing single bond and double bond …C=C−C… moiety, providing the migration of protons (tautomerization). (b) FF molecule with amino bond, providing high mobility of torsion angles (between atoms CB7, CA3, C5, N23, CA25) and dipole D_{FF}. (c) Formation of the molecular rings from 6 FF molecules joined by hydrogen bonds (H-bonds) between FF molecules. (d) Formation of tubular FF PNT structure joined by H-bonds between FF rings. The dashed lines denote the N−H…O H-bonding. Red, oxygen; deep blue, nitrogen; light blue, carbon; gray, hydrogen; yellow tubes, coil of amino bonding.
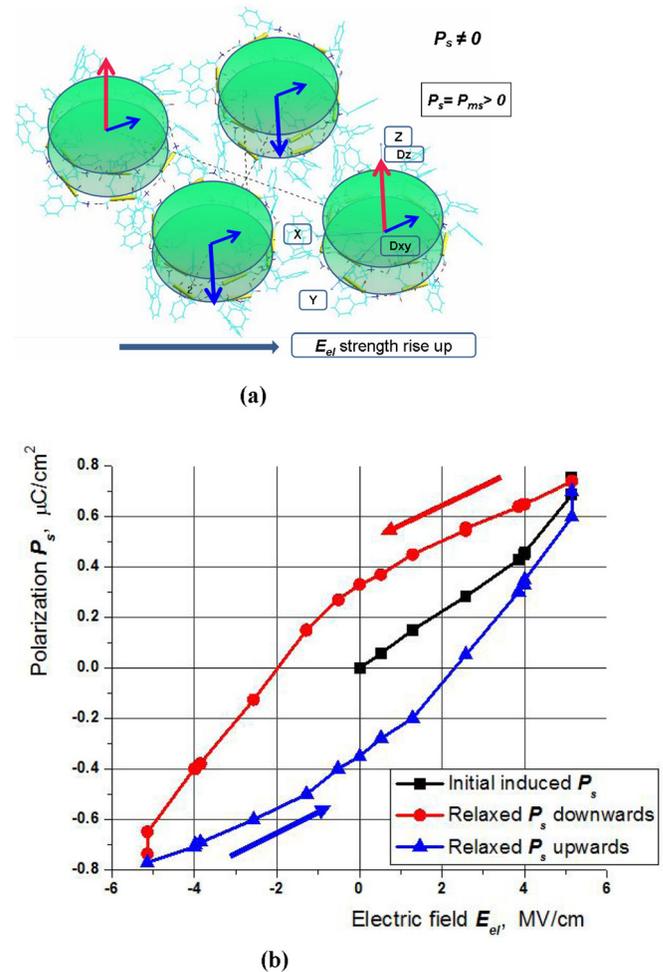

FIG. 7. Schematic illustration of the molecular model for individual FF tube bundles self-assembled after annealing at 150 °C (orthorhombic phase) with a fully compensated total dipole moment ($P_s = 0$) before poling, then during poling ($P_s \neq 0$) (a), and the resulting remanent polarization hysteresis loop under varying radial electric field E_{el} calculated in our model (b).

switching and thus proves the viability of the suggested mechanism.

Using our model, we could evaluate the value of the radial piezoelectric coefficient in the following way. The remanent polarization value P_s obtained via molecular modeling of FF PNTs is about 0.8 $\mu C/cm^2$. Further, the calculated polarizability α was estimated to be about 400 $\mathring{A}^3 \approx 45 \times 10^{-39}$ C m^2/V. This value leads to the estimated dielectric constant $\varepsilon \approx 4$ with the use of a Clausius-Mossotti equation. Though the dielectric constant of peptide nanotubes is still unknown, this value is consistent with the direct dielectric measurements of pressed nanotube pellets.[33] Optimization of the PNT structure under the applied electric field allowed evaluation of the volume change, and thus the electrostriction coefficient relating deformation and polarization could be also estimated in our model: $Q \approx 33$ m^4/C^2. Using these values, we could roughly estimate the expected radial piezoelectric coefficient via a simple linearized electrostriction equation (neglecting the apparent anisotropy of PNTs): $d_{radial} \sim 2Q\varepsilon\varepsilon_0 P_s$. This expression provides an approximation of the value of the longitudinal piezoelectric coefficient in peptide nanostructures: $d \sim 10$ to 15 pm/V. This value is in line with the experimental data measured on vertical PNTs

(Ref. [19]) and is comparable with the value extracted from Fig. 4(a) using $LiNbO_3$ crystal as a reference.[18] Further studies and calculations of the PFM contrast for anisotropic case[34] are currently in progress.

Using our modeling results and phenomenological theory, we could also estimate the expected size of polarization patterns under applied electric field. According to Molotskii,[26] the length l_o and lateral radius r_0 of the nascent polarization domain are determined via simple relations (see Fig. S3 and Annex S1 of the Supplementary Material[40]) involving the domain wall energy σ and effective force f acting on the domain wall by inhomogeneous electric field provided by a tip with radius R. For the calculations, we used domain wall energy values of $\sigma \sim 0.05$ to 0.2 mJ/m^2 based on the estimations from our model for the inter-tube FF condensation energy. In the calculations, we assumed that the nominal tip radius value $R = 10$ nm and the dielectric constant $\varepsilon \approx e_a = \varepsilon_c = 4$ (thus neglecting its anisotropy in the first approximation). Using the already mentioned Molotskii formalism[26] and neglecting the curved geometry of the tubes, we obtained a rough approximation of the diameter of the nascent domain in the range of 1000–2000 nm, with the

value being close to the experimental data shown in Fig. 5(b).

We also estimated the expected penetration depth of the electric field z_c using well-known phenomenological equations from Molotskii[26] and the minimal equilibrium size of the nascent domain in the case of PNTs (see also Annex S2 of the Supplementary Information[40]). Using the parameters set above, we calculated a z_c of about 25 nm for an applied voltage of 100 V. As the minimum external diameter of the tubes is about 50 nm [Fig. 1(a)], the artificial domain penetrates through the tube wall and could then be stabilized by the reduced depolarization field.[27] Our experimental data show that the threshold voltage for the formation of a stable polarized pattern could be as low as 30 V (Fig. 4). For this voltage, z_c is about 11 nm, which is several times greater than the minimal wall width estimated for the "single wall" PNT $r_{FF} \sim 25$ Å $= 2.5$ nm. This signifies that polarization domains can be, in principle, stabilized on the surface of very small nanotubes, thus making them potential candidates for the organic version of solid-state AFM-based ferroelectric memories.[35] The natural advantages of PNTs are their small diameter and absence of cross-talk in one dimension. Parallel arrays of the PNTs can be fabricated via the electrodeposition technique, as recently demonstrated by de la Rica *et al.*[36] Based on these calculations and the possible geometry of the parallel array of peptide nanotubes, we can theoretically access the maximum possible bit density of PNT-based organic memory. For a pattern diameter ~100 nm (poling voltage of 30 V), the memory density (per unit length) should be close to 10^7 m^{-1}. In this case, the depth of the artificial domain l_0 is in the range of 400–1000 nm and thus should penetrate into the tube cavity for PNTs having an external diameter of about 1000 nm.[26] It thus can be concluded that the possible density of a tube array consisting of parallel individual PNTs 1 μm in diameter is about 10^7 m$^{-1} \times 10^6$ m$^{-1} = 10^{13}$ m$^{-2} = 10^9$ cm^{-2} (i.e., 1 Gbit/cm^2). This is much less than what has been demonstrated in ferroelectrics by Samsung[37] (sub-10 nm bit size) and by Cho's group[38] in Japan (1.50 Tbit in.$^{-2}$) using non-linear dielectric AFM-based detection. Apparently, the storage density can be improved if smaller tubes are used for the fabrication of arrays. It should be noted that the abovementioned record storage parameters were obtained in inorganic materials containing heavy metals (e.g., Pb) and having high melting points and deposition temperatures. These are fully incompatible with modern organic/plastic electronics[39] and a tubular nanostructure can be important for the fabrication of high aspect ratio nanodevices. Even more prospects for the demonstrated polarization switching are expected in periodically poled optical devices in which such structures can be used, e.g., as all-optical switching components for second harmonic generation.

V. CONCLUSIONS

In this work, we describe local polarization switching that was observed for the first time by means of piezoresponse force microscopy in diphenylamine peptide nanostructures with tubular geometry. Annealed tubes exhibit radial polarization switching with a threshold voltage of about 30 V and polarization saturation at ca. 100 V, as evidenced by piezoresponse hysteresis loop acquisition. Molecular switching was modeled via a HyperChem program, and the results were compared with experimental data. Several important parameters were derived, such as the saturation polarization, coercive field, dielectric permittivity, electrostriction, and piezoelectric coefficient. The diameter of the switched polarized patterns was estimated using the Molotskii model, and the potential of PNTs as a media for dense ferroelectric memory was assessed. The discovered polarization switching in peptide nanotubes could be useful for future organic electronics.

[1]A. J. Lovinger, Science **220**, 1115 (1983).
[2]S. Das and J. Appenzeller, Nano Lett. **11**, 4003 (2011).
[3]S. Horiuchi and Y. Tokura, Nature Mater. **7**, 357 (2008).
[4]G. M. Whitesides, J. P. Mathias, and C. T. Set, Science **254**, 1312 (1991).
[5]V. Berl, I. Huc, R. G. Khoury, M. J. Krische, and J. M. Lehn, Nature **407**, 720 (2000).
[6]S. Zhang, Nat. Biotechnol. **21**, 1171 (2003).
[7]R. C. G. Naber, C. Tanase, P. W. M. Blom, G. H. Gelinck, A. W. Marsman, F. J. Touwslager, S. Setayesh, and D. M. Leeuw, Nature Mater. **4**, 243 (2005).
[8]E. Gazit, Chem. Soc. Rev. **36**, 1263 (2007).
[9]J. D. Hartgerink, J. R. Granja, R. A. Milligan, and M. R. Chadiri, J. Am. Chem. Soc. **118**, 43 (1996).
[10]S. Scanlon and A. Aggeli, Nano Today **3**, 22 (2008).
[11]M. Reches and E. Gazit, Curr. Nanosci. **2**, 105 (2006).
[12]E. Gazit, FASEB J. **16**, 77 (2002).
[13]C. H. Görbitz, Chem. Eur. J. **7**, 5153 (2001).
[14]C. H. Görbitz, New J. Chem. **27**, 1789 (2003).
[15]C. H. Görbitz, Chem. Commun. **22**, 2332 (2006).
[16]V. L. Sedman, L. Adler-Abramovich, S. Allen, E. Gazit, and S. J. B. Tendler, J. Am. Chem. Soc. **128**, 6903 (2006).
[17]N. Kol, L. Adler-Abramovich, D. Barlam, R. Z. Shneck, E. Gazit, and I. Rousso, Nano Lett. **5**, 1343 (2005).
[18]A. Kholkin, N. Amdursky, I. Bdikin, E. Gazit, and G. Rosenman, ACS Nano **4**, 610 (2010).
[19]A. Heredia, I. Bdikin, S. Kopyl, E. Mishina, S. Semin, A. Sigov, K. German, V. Bystrov, and A. L. Kholkin, J. Phys. D **43**, 462001 (2010).
[20]D. A. Bonnell, S. V. Kalinin, A. L. Kholkin, and A. Gruverman, MRS Bull. **34**, 643 (2009).
[21]A. L. Kholkin, A. V. Kalinin, A. Roelofs, and A. Gruverman, in *Scanning Probe Microscopy: Electrical and Electromechanical Phenomena at the Nanoscale*, edited by S. Kalinin and A. Gruverman (Springer, New York, 2006), Chapter 1, p. 173.
[22]M. Minary-Jolandan and M.-F. Yu, ACS Nano **3**, 1859 (2009).
[23]L. Adler-Abramovich, M. Reches, V. L Sedman, S. Allen, S. J. B. Tendler, and E. Gazit, Langmuir **22**, 1313 (2006).
[24]J. Ryu and C. B. Park, Biotechnol. Bioeng. **105**, 221 (2010).
[25]S. V. Kalinin, A. N. Morozovska, L.-Q. Chen, and B. J. Rodriguez, Rep. Prog. Phys. **73**, 056502 (2010).
[26]M. Molotskii, J. Appl. Phys. **93**, 6234 (2003).
[27]N. Pertsev, A. Petraru, H. Kohlstedt, R. Waser, I. Bdikin, D. Kiselev, and A. L. Kholkin, Nanotechnology **19**, 375703 (2008).

[28] A. L. Kholkin, A. K. Tagantsev, E. Colla, D. Taylor, and N. Setter, Integr. Ferroelectr. **15**, 317 (1997).

[29] S. V. Kalinin, B. J. Rodriguez, J. D. Budai, S. Jesse, A. N. Morozovska, A. Bokov, and Z.-G. Ye, Phys. Rev. B **81**, 064107 (2010).

[30] *Broadband Dielectric Spectroscopy*, edited by F. Kremer and A. Schonhals (Springer, Berlin, 2003).

[31] V. V. Shvartsman, A. L. Kholkin, M. Tyunina, and J. Levoska, Appl. Phys. Lett. **86**, 222907 (2005).

[32] HyperChem 7.52, *Tools for Molecular Modeling*, Hypercube, Inc., 2002.

[33] I. Bdikin, V. Bystrov, S. Kopyl, R. G. L. Lopes, I. Delgadillo, J. Gracio, E. Mishina, A. Sigov, and A. L. Kholkin, Appl. Phys. Lett. **100**, 043702 (2012).

[34] E. A. Eliseev, S. V. Kalinin, S. Jesse, S. L. Bravina, and A. N. Morozovska, J. Appl. Phys. **102**, 014109 (2007).

[35] T. Tybell, P. Paruch, T. Giamarchi, and J.-M. Triscone, Phys. Rev. Lett. **89**, 097601 (2002).

[36] R. de la Rica, C. Pejoux, and H. Matsui, Adv. Funct. Mater. **21**, 1018 (2011).

[37] D. C. Yoo, C. M. Lee, B. J. Bae, I. S. Kim, J. E. Heo, D. H. Im, S. H. Choi, S. O. Park, H. S. Kim, U.-In. Chung, J. T. Moon, B. I. Ryu, D. J. Kim, and T. W. Noh, in *Proceedings of the Electron Devices Meeting* (IEDM '06), San Francisco, December 2006.

[38] Y. Cho, K. Fujimoto, Y. Hiranaga, Y. Wagatsuma, A. Onoe, K. Terabe, and K. Kitamura, Nanotechnology **14**, 637 (2003).

[39] J. J. Brondijk, K. Asadi, P. W. M. Blom, and D. M. de Leeuw, J. Polym. Sci., Part B: Polym. Phys. **50**, 47 (2012).

[40] See supplementary material at http://dx.doi.org/10.1063/1.3699202 for models and calculation details.